2008 8th IEEE-RAS International Conference on Humanoid Robots
December 1 ~ 3, 2008 / Daejeon, Korea

Safe Joint Mechanism using Double Slider Mechanism and Spring for Humanoid Robot Arm

Hwi-Su Kim[1], Jung-Jun Park[1], Jae-Bok Song[1]

[1] *Korea University, Korea, fight704@korea.ac.kr, hantiboy@korea.ac.kr, jbsong@korea.ac.kr*

***Abstract*— In recent years, collision safety between a human and a robot has drawn much attention as service robots and humanoids are increasingly being used in the human environment. Safety of a robot arm can be achieved by either active or passive compliance system. Since active compliance systems with actuators are usually slow and expensive, several passive compliance systems with purely mechanical elements are proposed. Passive systems can provide faster response to collision and higher reliability than active systems. Since both positioning accuracy and collision safety are equally important, a robot arm should have very low stiffness when subjected to a collision force greater than the one causing human injury, but maintain very high stiffness otherwise. In order to implement these requirements, a safe joint mechanism composed of a linear spring, slider-crank mechanism, and 4-bar linkage is proposed in this research. Various experiments on static and dynamic collisions show high stiffness of the SJM against an external force of less than the pre-determined threshold force, but an abrupt drop in the stiffness when the external force exceeds this threshold, which guarantees positioning accuracy and collision safety.**

I. Introduction

In recent years humanoid robots and service robots have drawn a great deal of attention. Since these robots are operating in human environments, the safety issues related to physical human-robot interaction is increasingly important.

A safe robot arm can be achieved by either active compliance or passive compliance. In the actively compliant arm, collision is detected by a sensor, and the stiffness of the arm is lowered by appropriate control of joint motors. Since this approach involves sensing and actuation in response to dynamic collision, its bandwidth is rather limited. Moreover, the scheme of sensing and actuation inevitably results in high cost, sensor noise, and possible malfunction.

On the other hand, the passive compliance method consists of pure mechanical elements. Since this approach does not use any sensor or actuator, it can provide fast and reliable responses even for dynamic collision. Several mechanisms have been developed to achieve safety with passive compliance method. Some examples are the programmable passive compliance shoulder mechanism [1], the mechanical impedance adjuster with a leaf spring and an electromagnetic brake [2], a passive compliance joint with rotary springs and a MR damper [3]. A variable stiffness actuator with the nonlinear torque transmitting system composed of a spring and a belt was also developed [4].

A spring is by far the most popular mechanical element for shock absorption. However, the soft spring used at the arm joint leads to positioning inaccuracy because displacement occurs even for a small external force that does not require any shock absorption. Although a hard spring can provide high positioning accuracy of a robot arm, its capability of shock absorption is much lower than a soft spring, thereby giving higher probability of injury upon collision with humans.

To cope with this problem, a safe link mechanism and a safe joint mechanism using the nonlinear spring system were suggested in our previous research [5][6]. Those safety mechanisms can exhibit very low stiffness when subjected to a collision force greater than the one that may cause injury to humans, but can maintain very high stiffness otherwise. However, implementation of this safety mechanism for the humanoid arm requires more compact design.

In this research, the new design of the safe joint mechanism (SJM-II) is suggested for application to the humanoid robot arm. SJM-II is mainly composed of linear springs and a modified double slider mechanism. Springs are used to absorb collision force for safety, while the modified double slider mechanism determines the level of the external force so that the SJM operates only in case of a large external force. The main contribution of the proposed device is a significant reduction in size and weight in the realization of the nonlinear spring system.

The rest of the paper is organized as follows. The principle of operation and the structure of SJM-II is discussed in Section 2. Section 3 shows the proposed model of SJM-II. Various experimental results for both static and dynamic collisions are provided in Section 4. Finally, conclusion and future work is presented in Section 5.

II. Operational Principle and Construction of Safe Joint Mechanism II

As mentioned earlier, springs have been widely used for various safety mechanisms because of its good shock-absorbing property. However, a linear spring cannot be used directly in the robot arm because its displacement is proportional to the external force.

The robot arm equipped with soft springs exhibits deflection due to its own weight and/or a small load, as shown in Fig. 1. This characteristic is advantageous to collision safety, but causes low positioning accuracy. To cope with this problem, it is desirable to develop a spring whose stiffness remains very high when the external force acting on the end-effector of a robot arm is within the range of the normal operation, but rapidly drops when the force exceeds a certain level due to collision with the object. However, no such spring

978-1-4244-2822-9/08/$25.00 ©2008 IEEE

with this ideal feature does not exist. In this research, the nonlinear power transmission characteristics of a double slider mechanism are exploited to achieve this nonlinear spring feature.

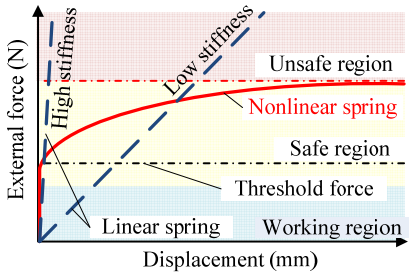

Fig. 1 Comparison between linear and nonlinear spring.

The robot arm equipped with soft springs exhibits deflection due to its own weight and/or a small load, as shown in Fig. 1. This characteristic is advantageous to collision safety, but leads to low positioning accuracy. To cope with this problem, it is desirable to develop a spring whose stiffness remains very high when the external force acting on the end-effector of a robot arm is within the range of normal operation, but rapidly drops when the force exceeds a certain level due to collision with the object. However, no such spring with this ideal feature does not exist. In this research, the nonlinear power transmission characteristics of a double slider mechanism are exploited to achieve this nonlinear spring feature.

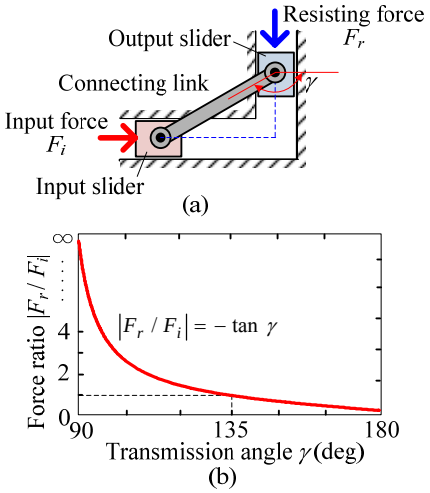

Fig. 2 Double slider mechanism: (a) simplified model, and (b) force ratio vs. transmission angle.

Consider a double slider mechanism shown in Fig. 2(a). When an input force F_i is exerted on the input slider in the x-axis direction, an appropriate resisting force F_r acting on point A of the output slider in the y-axis direction can maintain the static equilibrium of this mechanism. In the double slider mechanism, the transmission angle γ is defined as the angle between the connecting link and the line perpendicular to the output slider movement. The power transmission efficiency from the input to the output changes nonlinearly depending on this transmission angle, as shown in Fig. 2(b). As γ approaches 180°, much smaller F_r is sufficient to prevent the output slider from moving for a given F_i.

To achieve the nonlinear spring characteristic discussed in Fig. 1, the pre-compressed spring is installed between the output slider and the fixed wall. As shown in Fig. 3, the spring force F_s can offer the resisting force. At the zero configuration, the output slider is blocked by the fixed wall so that it cannot move downward from this zero position shown in Fig. 3. Since the resisting force caused by spring compression exists, the output slider does not move upward until the input force exceeds a certain threshold. This force required to initiate upward movement of the output slider is defined as the *threshold force*. Once the input force exceeds this threshold, the spring is rapidly compressed until it can no longer be compressed, which moves the output slider upward.

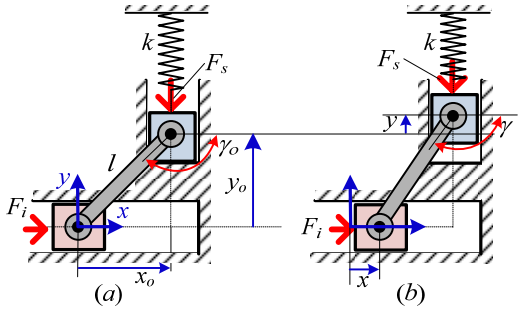

Fig. 3 Double slider mechanism with spring for realization of nonlinear stiffness: (a) zero configuration, and (b) general configuration.

The threshold force can be described by

$$F_{th} = -\frac{F_s}{\tan\gamma_o} = -\frac{k\,s_o}{\tan\gamma_o} \tag{1}$$

where the subscript o represents the zero configuration, s_o is the spring compression, γ_o is the transmission angle at the zero configuration, and k is the spring constant.

In Fig. 3(b), the input force F_i can be described by

$$F_i = k_{eq}\,x = -\frac{F_s}{\tan\gamma} = -\frac{k(s_o + y)}{\tan\gamma} \tag{2}$$

where k_{eq} is the equivalent stiffness seen from the input slider, x and y are the displacements of the input and output sliders, respectively.

The output slider displacement y can be described in terms of the input slider displacement x as follows:

$$y = \sqrt{l^2 - (l\cos\gamma_o + x)^2} - l\sin\gamma_o \tag{3}$$

with the length of the connection link l. The stiffness k_{eq} of this nonlinear spring system can be described by

$$k_{eq} = -\frac{k(s_o + y)}{x \tan\gamma}$$
$$= -\frac{k}{x}\left\{\frac{s_o + \sqrt{l^2 - (l\cos\gamma_o + x)^2} - l\sin\gamma_o}{\sqrt{l^2 - (l\cos\gamma_o + x)^2}\,/\,(l\cos\gamma_o + x)}\right\} \quad (4)$$
$$= -\frac{k}{x}\left\{l\cos\gamma_o + x + \frac{(l\cos\gamma_o + x)(s_o - l\sin\gamma_o)}{\sqrt{l^2 - (l\cos\gamma_o + x)^2}}\right\}$$

Figure 4 shows the equivalent stiffness curve as a function of displacement of the input slider. The stiffness of this system is kept very high for a small displacement of the input slider, but it quickly drops as the displacement increases. Hence this nonlinear stiffness can be realized by the double slider mechanism combined with a pre-compressed linear spring.

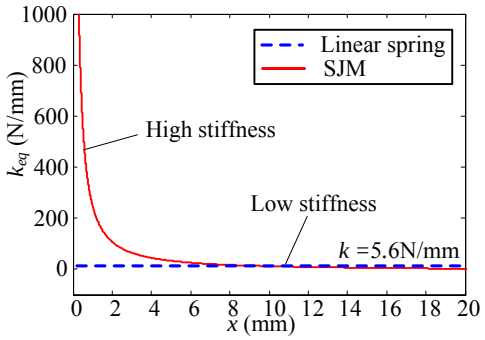

Fig. 4 Nonlinear stiffness of SJM as a function of displacement.

III. Model of Safe Joint Mechanism II

This section discusses the design of SJM. Section A presents selection of the spring stiffness, and section B deals with the prototype of SJM-II.

A. Selection of spring stiffness

The threshold force of SJM-II can be set by adjusting the stiffness and initial compression of the spring and the initial transmission angle. It is noted that the threshold force should be larger than the desired payload of the robot arm for positioning accuracy.

As shown in Fig. 5, SJM-II is installed at the elbow joint of the 6 DOF humanoid arm which has a payload of 2kg. The length between the elbow joint and the end-effector is 344 mm, weight is 0.7 kg and the maximum speed and acceleration of the end-effector is 1 m/s and 3.5 m/s^2, respectively.

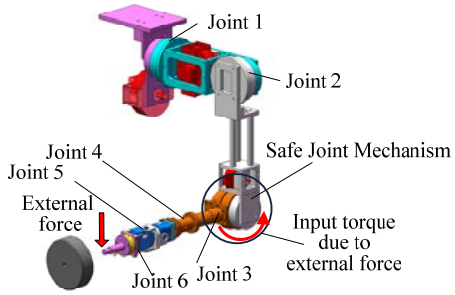

Fig. 5 6 DOF humanoid arm with safe joint mechanism.

Dynamic simulation was conducted to evaluate the torque required for the elbow joint satisfying the above conditions. The humanoid is simulated in the extreme situation that is operated at the maximum velocity and acceleration. Figure 6 shows that the maximum required torque is 10 Nm in the dynamic motion of the robot arm. Therefore, the threshold force should be set to a larger value than this maximum torque.

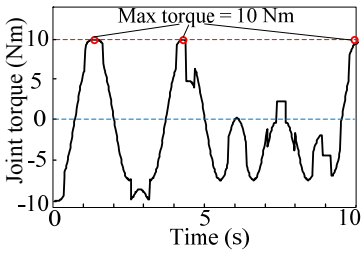

Fig. 6 Torque required for joint 3 in dynamic operation.

Figure 7 shows the modified double slider mechanism in which a crank is added to transmit input torque. As shown in the figure, since the arm is composed of revolute joints, the external force acting on the end-effector of the arm is converted into the input torque at each joint. This input torque T_i causes the input force F_i by the crank. Therefore, the threshold force causing a drastic change in joint stiffness can also be described in terms of the threshold torque.

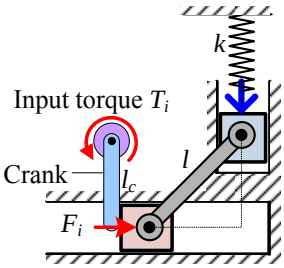

Fig. 7 Modified double slider mechanism with spring.

From the geometric parameters of the mechanism and the threshold torque, the spring stiffness can be given by

$$k \geq \left| 0.9 \times \frac{T_{th}}{l_c \cdot s_o} \times \tan\gamma_o \right| \quad (5)$$

where T_{th} is the threshold torque generating the threshold force, l_c is the crank length, and s_o is the spring compression at the zero configuration. Note that the friction coefficient of 0.9 is included for various types of friction in the unit. In this analysis, $\gamma_o = 169^\circ$, $s_o = 12$ mm, $l_c = 26$ mm, which yields $k = 5.6$ N/mm. This model adopts two springs of $k = 2.8$ N/mm so as to acquire enough compression of a spring.

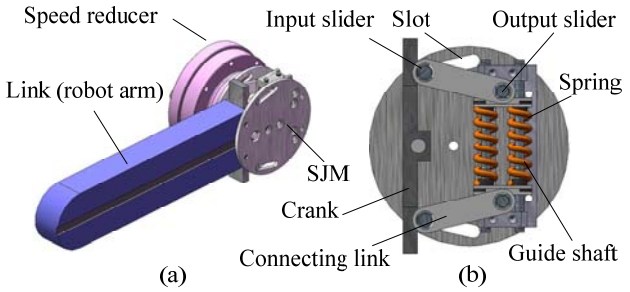

Fig. 8 Model of SJM-II; (a) installation of SJM-II at joint 3, and (b) structure of SJM-II.

As shown in Fig. 8(a), SJM-II is installed at the non-backdrivable speed reducer and the robot link is connected to the crank. Collision force can be transmitted to the modified double slider mechanism of the SJM-II by means of the crank rigidly connected to the robot link. Therefore, the collision force does not affect the speed reducer and the motor directly. The input slider of the SJM-II moves inside the inclined guide slot. Furthermore, the two modified double slider mechanisms are arranged symmetrically so that they can absorb the collision force applied in both directions.

The optimal motion of this system can be achieved, which means small displacement of the output slider can lead to large angular displacement of the crank, so that the size of the SJM-II can be reduced. In order to prevent plastic deformation of the spring, the motion range of the output slider is limited by the slot geometry.

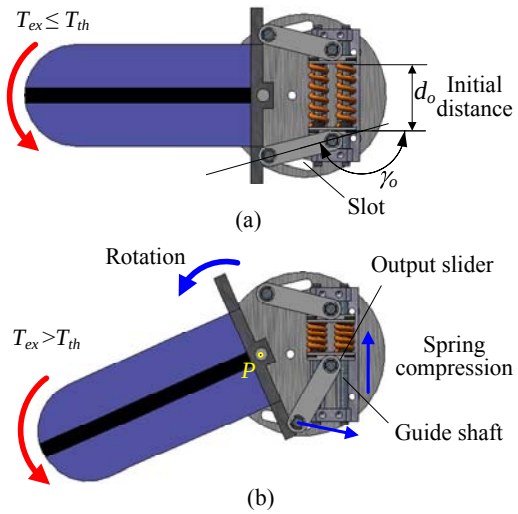

Fig. 9 Operation of SJM-II with external force; (a) before collision, and (b) after collision.

When the input torque T_i from the external torque T_{ex} is smaller than the pre-determined threshold torque T_{th}, the SJM-II provides stiffness high enough to maintain the static equilibrium, which prevents rotation of the link. However, if the input torque exceeds the threshold torque, then the crank turns around point P, as shown in Fig. 9(b) and then the output slider is forced to move up on the guide shaft to compress the spring. This movement of the output slider reduces the transmission angle, so sustaining the static balance requires a greater resisting force for the same input force. However, the increased spring force due to its compression is not large enough to sustain this balance. This unbalanced state causes the slider to rapidly slide up. As a result, the collision force can be absorbed by the spring compression.

The prototype of the SJM-II was constructed to conduct various experiments on its performance, as shown in Fig. 10. The diameter of SJM-II is 70mm, the height and weight are 35 mm and 180 g, which are smaller and lighter than the previous version (ϕ75*50 mm, 400 g) [6].

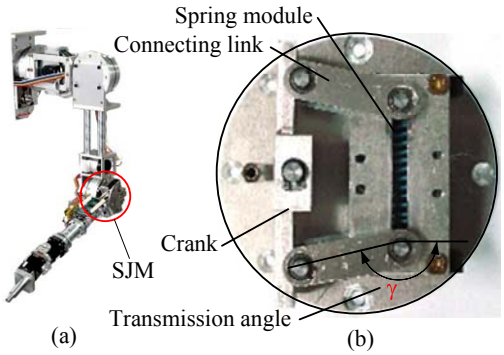

Fig. 10 Prototype of SJM-II; (a) humanoid arm with SJM-II, and (b) construction of SJM-II.

IV. Experiments for Safety with Safety Mechanism.

This section presents some experiments conducted to verify the performance of SJM-II when the robot arm collides with a human.

Since there are no clear safety criteria associated with the collision between a manipulator and a human, several different criteria have been applied to the evaluation. However, most criteria were suggested for the industrial manipulator, and thus they are not suitable for application to the humanoid robot arm. Therefore, it is important to find appropriate criteria for the humanoid robot. In this research, the contact force is applied to measure the collision safety of the humanoid robot arm with and without the proposed SJM-II.

In the experiments on static collision, the human pain tolerance of 50 N was used as the threshold force [7]. In case of the experiments on dynamic collision, the collision force between the robot arm and the wall is used as a criterion to verify the effect of the SJM-II.

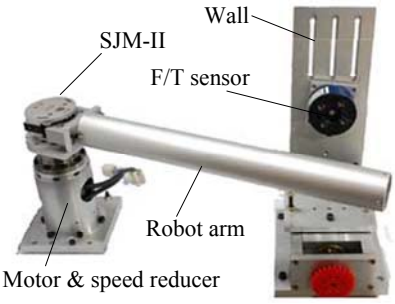

Fig. 11 Experimental setup for 1 DOF robot arm with SJM-II.

For evaluation of collision safety with and without SJM-II, the experiment setup shown in Fig. 11 was designed. The SJM-II is installed at the 1-DOF robot arm which has a similar weight and length to the humanoid robot arm shown in Fig. 10. The plate of SJM-II integrated with the 1 DOF robot arm is attached to the gear reducer which is connected to the motor. Therefore, the torque of a motor can be transmitted to the robot arm via the SJM-II and the gear reducer. The F/T sensor is installed at the wall to measure the contact force between the robot arm and the wall.

The experiment on static collision was conducted to measure the minimum operational force of the SJM-II. The end-point of the robot arm was initially placed to barely touch a fixed wall, and its joint torque provided by the motor was gradually increased. The static contact force between the robot link and the wall was measured by the F/T sensor. Experiments were conducted for the robotic arms with and without the SJM-II.

The robot arm without SJM-II delivered a contact force of up to 80N to the wall, which was well above the critical contact force of 50N, as shown in Fig. 12. However, the contact force of up to only 27N was transmitted to the wall with SJM-II. It means that the contact force does not exceed the threshold force to cause the pain because the excessive force is absorbed by the SJM-II.

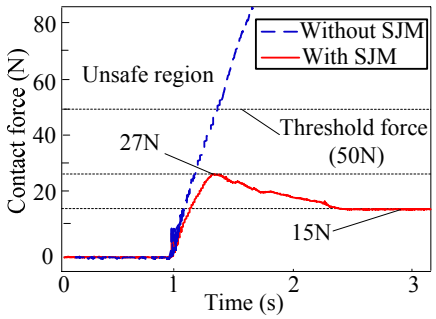

Fig. 12 Experimental result of static collision

The experiments on dynamic collision was conducted to investigate the collision safety of the humanoid robot arm with and without the SJM-II. In this experiment, the end-point of the robot arm collided at a constant velocity of 2 m/s. To press the wall continuously after collision, the robot arm was commanded to reach the desired position which was placed 5 cm inside the wall. Experiments were conducted for the robot arm with and without the SJM-II.

In Fig. 13(a), the collision force at the wall reached 457N without SJM-II. With the SJM-II, however, the maximum collision force was 307N, as shown in Fig. 13(b). Also, the collision force with the SJM-II after collision was lower than that without it.

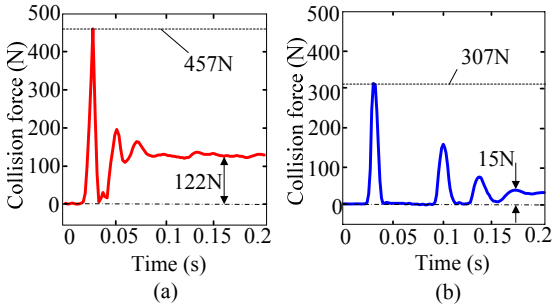

Fig. 13 Experimental results on dynamic collision; (a) without SJM-II, and (b) with SJM-II.

V. Conclusions

In this research, the safe joint mechanism II (SJM-II) was proposed for collision safety. The robot arm equipped with the SJM-II can maintain very high stiffness up to the preset threshold force, but provides a very low stiffness above the threshold. From the analysis and experiments, the following conclusions are drawn:

1) Stiffness of the robot manipulator abruptly drops if the external force exceeds the pre-determined threshold force. Therefore, collision safety can be achieved when the robot works in human environments.

2) High stiffness of the robot arm can be maintained for low external force less than the threshold force. Therefore, positioning accuracy can be achieved for the tasks involving low external forces.

Currently, the research on more compact design of SJM-II is in process.

Acknowledgements

This research was supported by the Personal Robot Development Project funded by the Ministry of Knowledge Economy of Korea and the Korea Science and Engineering Foundation (KOSEF) grant (No. R11-2007-028-01002-0).

References

[1] M. Okada, Y. Nakamura and S. Ban, "Design of programmable passive compliance shoulder mechanism," *Proc. of the IEEE International Conference on Robotics and Automation*, pp.348-353, 2001.

[2] T. Morita and S. Sugano, "Development of one-D.O.F. robot arm equipped with mechanical impedance adjuster," *Proc. of the IEEE/RSJ International Conference on Intelligent Robots and System*, pp. 407-412, 1995.

[3] S. Kang and M. Kim, “Safe Arm Design for Service Robot,” *Proc. of the International Conference on Control, Automation and System*, pp.88-95, 2002.

[4] G. Tonietti, R. Schiavi and A. Bicchi, “Design and Control of a Variable Stiffness Actuator for Safe and Fast Physical Human/Robot Interaction,” *Proc. of the IEEE International Conference on Robotics and Automation*, pp. 528-533, 2005.

[5] J.-J. Park, B.-S. Kim and J.-B. Song, “Safe Link Mechanism based on Passive Compliance for Safe Human-Robot Collision,” *Proc. of the IEEE International Conference on Robotics and Automation*, pp. 1152-1157, 2007.

[6] J.-J. Park, Y.-J. Lee, J.-B. Song and H.-S. Kim, “Safe Joint Mechanism based on Nonlinear Stiffness for Safe Human-Robot Collision”, *Proc. of the IEEE International Conference on Robotics and Automation*, pp. 2177-2182, 2008.

[7] Y. Yamada, Y. Hirasawa, S.Y. Huang and Y. Umetani, “Fail-safe human/robot contact in the safety space,” *IEEE International Workshop in Robot and Human Comunication*, pp.59-64, 1996.